Comparative Analysis of LBP variants

Gousiya Habib
Department of Computer Science
National Institute of Technology
Srinagar, India
gousiahabib_01phd19@nitsri.net

Shaima Qureshi
Department of Computer Science
National Institute of Technology
Srinagar, India
shaima@nitsri.net

Abstract: Texture is an essential characteristic of the visual patterns appearing in natural surfaces and images. The local binary pattern has a wide variety of applications ranging from texture classification (histopathological images, remote sensing images to image segmentation (biomedical imaging). Many proposed feature descriptor methods that are easy to implement have low performance while as other methods are not able to improve even by modifying using various transforms like translation, rotation, affine and perspective transform. Local binary patterns (LBP) have come forth as one of the extensively studied descriptors for texture type. Although extensive research has been carried out using LBP in industrial inspection, facial recognition, character recognition, it, however, remains open for further work mainly in the medical area. Paper first describes texture classes in detail with spcial focus on LBP. A comparative analysis of various rotation is performed on a medical data set. provides a detailed description of Local binary patterns and comparative analysis of various rotation invariant variants of LBP in terms of classification accuracy of medical images.

Keywords—Local Binary Pattern, Texture Classification, Histogram of equivalent pattern, SLBP

I. Introduction

Texture is a natural property of elements or scenes, which owns the traits of brightness, shade, shape, scale, and many others, etc. Texture analysis is an area of broad research. The evaluation of 2-D textures has numerous suitable applications, for instance, in defect detection, remote sensing, and biomedical image analysis, however, there is solely a restrained number of examples where its flourishing exploitation has been done. The principle inconvenience is that textures in the actual world are not uniform because of variations in direction, scale or distinct visual appearance. The central issue of texture classification is to deal with the modifications in texture appearance to build robust and discriminative texture representation. The dark -scale invariance is regularly significant because of irregular brilliance or outstanding intra-class variableness. Moreover, the degree of computational complexity is huge for the majority of the proposed texture descriptors. Therefore the advancement of prevailing texture measures that can be extracted and classified within feasible computational complexity is the need of the hour. Local binary patterns (LBP) have risen as one of the most outstanding and broadly examined local texture descriptors. A beneficial texture feature, an essential constituent of texture categorization, is anticipated to accomplish two contending goals: low computational complexity, to allow the categorization errand to work in real-time; and catching the most democratic texture statistics of a texture class, such that dissimilar texture classes can be discerned in spite of the presence of numerous imaging aberrations (containing illumination, rotation, the viewpoint, scaling, occlusion, and noise). This paper discusses in detail the various texture classes with focus on the statistical approach.

All the existing, as well as recent versions of the statistical approach LBP, are discussed in this paper with their corresponding advantages and limitations. To evaluate the classification performance as well as computational time complexity, LBP and all the variants of LBP are implemented on publicly available medical image data set 2D-Hela. Performance comparison is done among all the variants of local binary patterns and relevant conclusions are drawn. Texture features can be classified into many families, like a statistically based approach, a structural based approach, Transform based approach, a Model-based approach, etc. which are depicted in Table1 (texture survey table). Section I gives the general introduction about texture features. and section II describes textuie classes in detail

II. Texture Classes:

A) Structural Features

The basic approach of the structural feature technique is to divide large textural components into simpler ones. These simpler components are regarded as texels or primitives, which always occur in some regular or recurrent order. Therefore, structural texture features are given by those texels or primitives and their corresponding spatial layout. The basic difference between structural texture approaches is how topic up these primitives. These texels can be as fundamental as individual pixels [1], a vicinity with uniform gray levels [2], or line fragments [3] edge separation in different orientations [4] edge repetition in different orientation [5]. Structural arrangements can be also considered as periodic associations of ‘lines’, ‘fragments’ and ‘line segments’ [6]. In 1976 Zucker et. al. recommended that common textures can be dealt with as perfect example

Figure-1: Detailed list of texture methods.

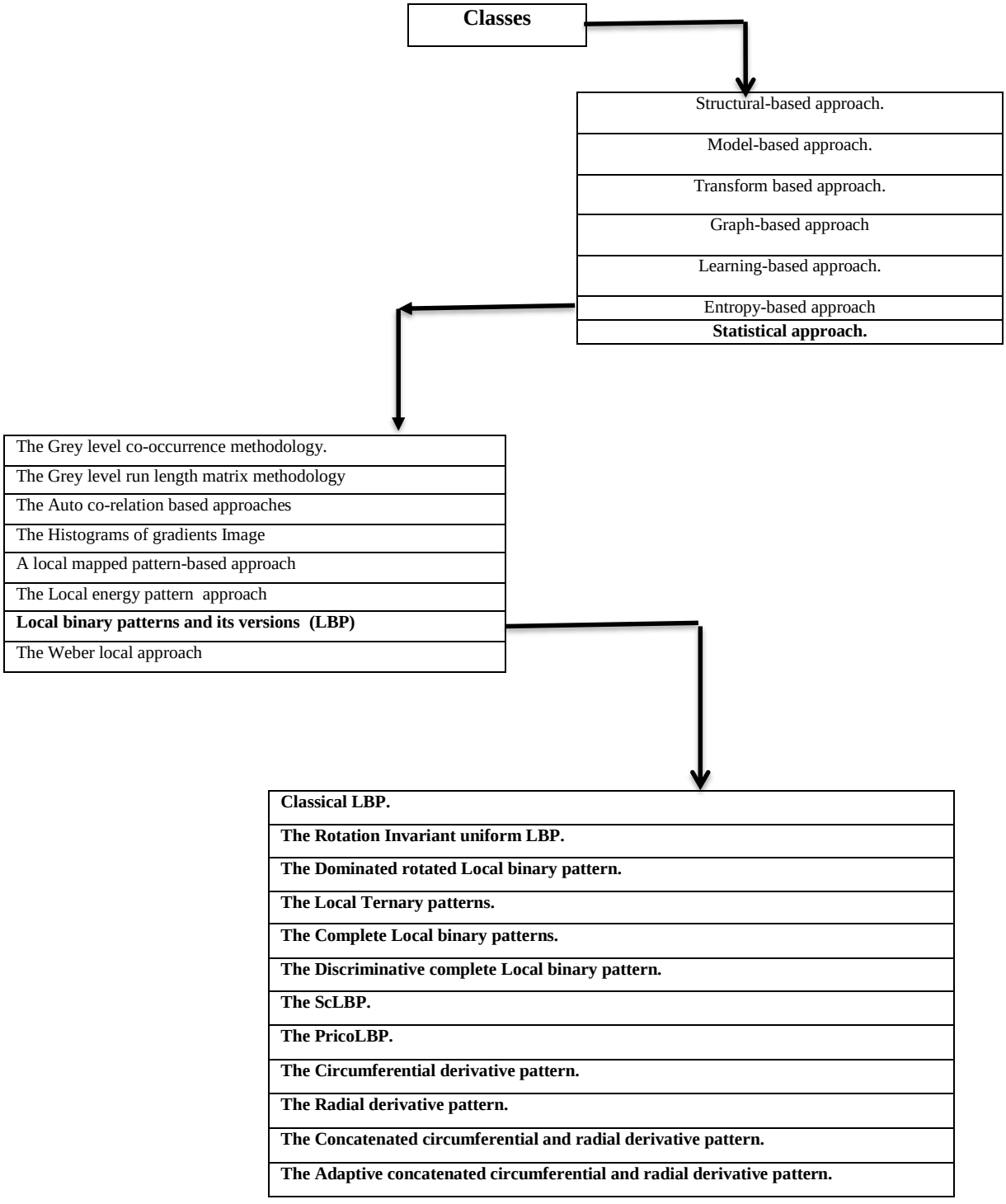

C) Transform based approach

The majority of signal processing based aspects are reliably expelled via applying filter banks to images and handling the vitality of the filter responses. These features can be procured from the spatial space, the repeated space, and the joint spatial spatial-repeat space. Gradient filters are applied to extract edges, lines, confined specks and other features from images in the spatial domain. Sobel, Robert, Fourier, Laplacian transformation based filters, Gabor decomposition-based filters [13], wavelet-based transform filters, the shearlet [14] transform-based filters and the Laws filters [15] have been routinely utilized as an antecedent to measuring edge thickness In 2017 Dong et al. [16] explore the concept of wavelets based on the same ground the proposed rotation invariant portrayal of texture components by utilizing multi-scale sampling. Later on in 2018 yang et al. [17] link complex wavelet transform and LBP for invariant texture classification (rotation invariance, brightness invariance, scale invariance).

The central issue in this method is that these spatial filter techniques are not able enough to deal with issues like noise and their counterparts that use information in the frequency domain.

D) Graph-based approach

Given an $n \times n$ input image represented by a graph of points. The highlights of these graphical structures can be obtained from the texture in the local graph neighborhood [18]. Thus feature extraction of image for these graph-based approaches relies completely on the graph obtained from the given input n*n image. This approach is also divided into different families like Local graph structures [19], Graph of tourist walk approach [20] shortest paths in graph methods based on graph theory [21].

One of the central issues of this approach is that graphical information is local, contains information about local patterns (micropatterns) and lacks global information, information about global patterns (macro patterns). Shift invariance and scale invariance [18] are some of the major drawbacks of this approach. Also, this approach is insensitive to image aberrations like illumination and rotation invariance.

E) Learning-based approach

The texture feature extraction methods depend upon the learning-based methods like vocabulary learning method, machine learning methods, deep learning methods The two vocabulary based methods like K-Means clustering and Gaussian Mixture Models use clustering approaches to extract features from the input data and thus making the cluster constituting a group of local descriptors in the feature vector. Therefore, these methods don't learn features directly from the training dataset. In 2010 Crosier and Griffin (22] investigated ideas based on the statistical methodology that represents an image as histograms over a feature set. The technique depends on Basic image features (BIFS) and doesn't rely upon a vocabulary learning based on clustering. Crosier and Griffin [22] proposed a framework satisfying the property of scale invariance and extracted features set from this designed framework exhibhit the properties of rotation invariance and image invaraiance. Later on, in 2013 Zhang et al. [23] implemented two local descriptors that possess the property of rotation invariance. Deep learning-based models like CNN are more efficient as they contain multiple convolutional layers that convolve the n*n image through k kernels to extract features from the entire input image.

These learning-based approaches are data-dependent (vocabulary-based learning) and as the deep learning-based methods (CNN) are data-hungry models, so they require large training sets hence are computationally very expensive. Also implementing these deep learning-based methods requires costly hardware (GPU's etc.) and infeasible because of this requirement.

F) Entropy-based approach

To process time-series data (*n*-dimensional data). Entropy-based methods are proven to be very useful in processing such data like time series data in biomedical imaging, time-series data in banking and finance and technology and engineering aspects. Various dimensional based on ID entropy approach for extracting texture features. In 2011 Yeh et al. [27] and 2016 Silva et al. [28] explored the idea of bi-dimensional sample entropy to measure irregularity in pixels patterns.

The strategy is in effect delayed as far as calculation time is concerned, subsequently the technique is computationally time inefficient strategy, and these methods give unreliable results for smaller sized images. The method is too sensitive to image aberrations like image rotation.

G) Statistical based approach

Spatial scattering or dispersion of pixels of the image represents statistical texture features. These pixels are all around built up in computer vision and have been broadly linked to different assignments. The picture histogram is a first request statistical component that is not just computationally straight-forward, yet besides pivot and interpretation invariant; it is in this manner normally utilized as a part of different vision applications, e.g. image ordering and recovery. Second arrange measurements look at the connection between a couple of pixels over the image space, for instance through autocorrelation. The fundamental inspiration driving these techniques depends upon authenticity that the human visual framework utilizes statistical highlights to recognize the textured neighborhood. The technique Local Binary Patterns (LBP) devised by Ojala et al. [29] proved one of the successful statistical technique.

i) Local binary pattern (LBP)

The LBP operator has emerged as a positive way of texture description. The traditional model of LBP operator processes the pixels of a concerning image through evaluating the 3×3 neighbourhood of each pixel towards center pixel value [30]. The ensuing threshold cost is summed up via

powers of two. Afterwards, the histogram of these labeled pixels serves as a texture descriptor. Mathematically formulation of LBP descriptor at the central pixel is given as:

$$LBP_{P,R} = \sum_{p=0}^{P-1} s\left(g_p - g_c\right)2^p$$

Where,

$$s(x) = \begin{cases} 1, \text{if } x \geq 0 \\ 0, \text{if } x < 0 \end{cases}$$

g_c and g_k represents the gray values of p_c (central pixel) and p_k, $k = (0,1,2,\ldots,P-1)$ represent corresponding neighbors. The g_c and g_k coordinates are given as $(0,0)$ and $\left(-R\sin\left(\frac{2\pi p}{P}\right), R\cos\left(\frac{2\pi p}{P}\right)\right)$. The framework of classical LBP operator is given as follows:

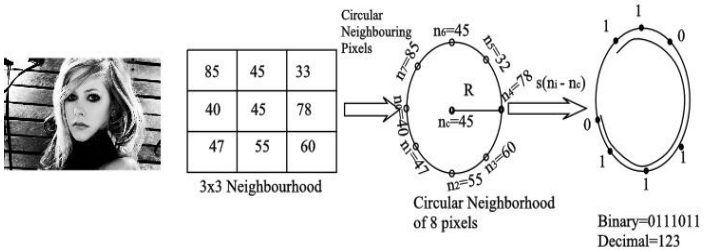

Fig. 1: Central pixel and its n circularly neighbors with radius R

The LBP operator has the functionality to cover the circular neighbourhoods of a range of sizes. The circular neighborhood of pixels and bilinear interpolation of pixels prompts major advantage of utilizing variable range neighborhood and variable radius. For circular neighborhoods. (P,R) represents *P* sampling points with radius *R* on the circumference of the circle.

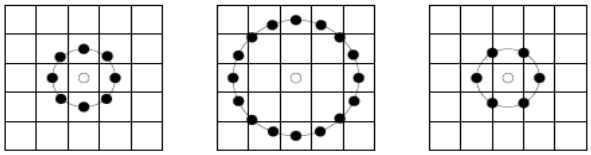

Fig. 2: Circular neighborhoods: (8, 1), (16, 2) and (6, 1).

Given the texture image of size $N \times M$, the LBP pattern $LBP_{r,p}(c)$ calculated at each pixel *c* in such a way that the textured image obtained comprises uniform distribution of LBP patterns followed by LBP histogram vector *h* representing the whole image.

$$h(k) = \sum_{i=1}^{N}\sum_{j=1}^{M} \delta\left(LBP_{r,p}(i,j) - k\right)$$

Where $0 \leq k < d = 2p$ represent number of LBP patterns. By simply swapping values of *P* and *R*, LBP features can be easily computed for any quantization of angular space and spatial resolution. The standard LBP feature extraction process is given in fig-3:

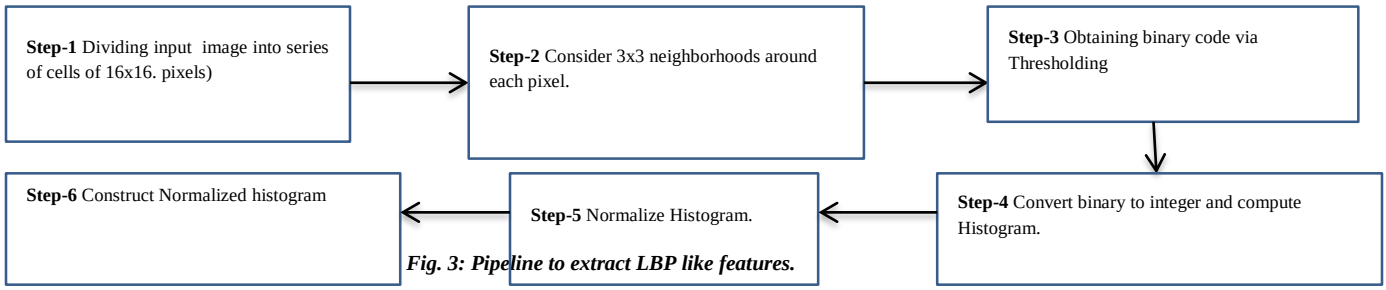

Fig. 3: Pipeline to extract LBP like features.

Among the various steps mentioned in Fig. 3, the first and fifth steps are problem-specific, in that, they rely upon the problem characteristics.

Preprocessing: There is no requirement of preprocessing in LBP. Features are obtained immediately from the input image.

***Neighborhood*:** Some pattern of pixels from an image is selected, which is sampled to compute local feature vectors.

Thresholding: Some threshold is chosen and binarization is performed to many levels.

Encoding and regrouping: to improve peculiarity, different methods are defined and combined.

Feature combination: Multiple complementary LBP-like descriptors are blended or non-LBP and LBP-like combo is performed Many LBP like complementary descriptors are blended or non-LBP and LBP-like combo is performed. LBP endures quite a few principal issues. An increase in local size prompts a simultaneous exponential increment in the number of patterns. LBP and its versions are now no more resistant to noise, image rotation. Moreover, it can seize only the neighborhood shape of the texture and fails to become aware of the massive scale texture structures. Ojala et al. [29] determined LBP patterns that are unique; represent the most important characteristics of the texture, provide the mass (around 90%) of a large number of patterns. These patterns regarded as uniform patterns other patterns as non-uniform patterns. The standard property of uniform patterns is that there are only two spatial transitions in the binary sample between 0 and 1 (property of being uniform in nature). And the same measure is given as:

$U(LBP_{P,R}) = \left|s\left(t_{P-1} - t_c\right) - s\left(t_0 - t_c\right)\right| + \sum_{p=1}^{P-1}\left|s\left(t_p - t_c\right) - s\left(t_{p-1} - t_c\right)\right|$ Moreover, $LBP_{P,R}^{riu2}$ execution can be further enhanced by acquiring rotation invariant variance measure $VAR_{P,R}$ that portrays the contrast of local image texture. These patterns which are rotation invariant uniform belongs to the class of uniformity of two or less and are given as:

$$LBP_{P,R}^{riu2} = \begin{cases} \sum_{p=0}^{P-1} s\left(t_p - t_c\right)2^p, \text{ if } U\left(LBP_{P,R}\right) \le 2 \\ P+1 \qquad\qquad \text{, otherwise} \end{cases}$$

$LBP_{P,R}$ to $LBP_{P,R}^{riu2}$ mapping results in feature dimensionality reduction of histogram representation having $P+2$ distinguishable values, from a pool of 2^p elements. And all the non-uniform patterns are combined in a single bin under the label $P+1$.

Advantages and Limitations

LBP is effective and robust and is demonstrating to be a powerful differentiator in many medical image classification problems. The classifiable rewards of LBP are its simplicity of execution, invariability to monotonic brightness alterations, low computational complexity and no need for pre-training. The original LBP suffers from various drawbacks, it generates not only too long but devastatingly large even for small regions, contributing to the diminished peculiarity and large memory utilization. The method is only able to detect local structures (microtextures) and unable to detect large-scale texture structures (macro textures).senstiveness to image aberrations like image rotation and image noise. In 2008, Unay and Ekin utilized LBP for texture analysis as a powerful nonparametric strategy. They utilized LBP for the extraction of helpful data from medical images, especially, from MRI of the brain.

ii) Uniform Local binary pattern (ULBP)

Due to the sensitiveness of LBP to image aberrations like rotation and noise, it was natural to refine the feature vectors without loss of any kind of essential information. Thus uniform LBP (ULBP) has at most two transitions from 0 to 1.

Advantages and Limitations

The choice of selection of uniform LBP over LBP helps in reducing the length of the feature vector and improves the performance of LBP feature classifiers. Although it reduces feature dimension, but not to acceptable still there is a need to reduce the feature dimensionality further also the variant is sensitive to rotation invariance.

iii) Rotation invariant Uniform Local binary pattern (R_iLBPU)

Method proposed by Ojala et al. [29] defined LBP with uniformity measure U. $LBP_{P,R}^{riu2}$ lowers feature dimensionality by classifying all 2^p LBP's into $P+2$ distinct groups.

The circular neighborhood is an essential condition for obtaining rotation invariance.

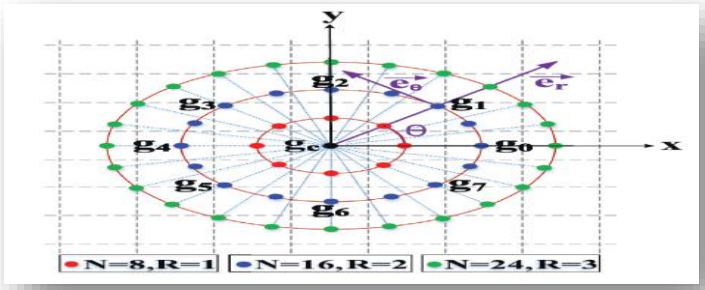

Fig. 4 Circular symmetric neighborhood for distinct (N, R) values

This symmetric circular neighborhood consists of *N* smooth points in a pixel equally aligned by an angle of $\frac{2\pi}{N}$ and at an equal distance of radius R from the pixel. *P* denotes set of points and are given by :

$$P = (p_n) \text{ where } p_n = \cot\left(\frac{2\pi\, n}{N}\right).$$

In 2002, Ojala et al. [29] devised the method for texture classification possessing the property of rotation invariance and scale invariance for multiple resolution dark-scale images. This method applied to greyscale and rotation invariant LBP based texture classification method. This method was only tested on dark-scale images and is not insensitive to noise.

Advantages and Limitations:

R_iLBPU as an extension of LBP is very well suited for greyscale images and is a fundamental property of all texture-based methods and possesses rotation invariance property. R_iLBPU is capable to analyze only smooth patterns that represent total binary patterns. Although it contains the central structure of texture information, but it still lacks the crucial data that is present in non-uniform patterns which leads to deterioration of performance. It also tends to lose spatial information gradually. Also, the problem with uniform LBP's features extracted from images may contain some of the patterns that need not be necessarily dominant like high curvature edges, crossing boundaries, or corners.

iv) Dominant Rotated Local Binary Pattern (DRLBP)

The issue of rotation invariance in LBP emerges because of the rigid arrangement weights. To counter the effects of rotation in the descripted calculation for an image, the rotations should be applied similarly to weights as well. Since the rotation angle can't be known. Rakesh Mehta et al. [30], proposed a versatile game plan of weights because of the locally figured deference direction. The main motive is that the deference direction must possess the same rotation angle as experienced by image rotation. And is taken as a reference direction, given by the following equation.

$$D = \underset{p\in(0,1,\ldots,P-1)}{\arg\max} \left| g_p - g_c \right|$$

The maximal difference of neighboring pixels concerning the central pixel. The technique quantifies the dominating direction into P discrete values. Rotated Local Binary Pattern (RLBP) is calculated by performing the rotation of weights as per given dominant direction. The weights are assigned as per the deference (which is the dominant direction in this case) in the circular neighborhood. In this way, RLBP administrator is characterized as:

$$RLBP_{P,R} = \sum_{p=0}^{P-1} s\left(g_p - g_c\right) 2^{\mathrm{mod}(p-DP)}$$

where $2^{\mathrm{mod}(p-DP)}$ represents weight term and mod represent the modulus operator. This weight term is dependent on D. Therefore mod operator gives the circular shift to the weights concerning the dominant direction, while keeping the sequence of weights the same. This circular shifting of weights prompts rotation invariance, as now weighs no more remain dependent on pre-chosen arrangement rather than they depend now only on the neighborhood.

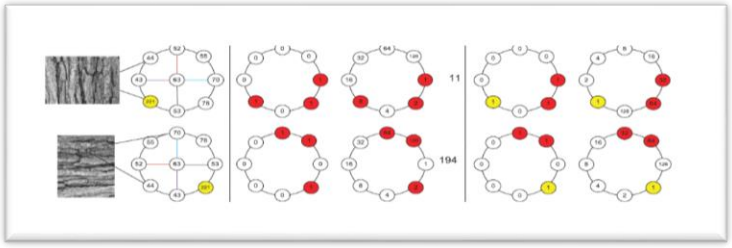

Fig. 5: The effect of rotation on LBP and RLBP operator.

In 2009 Liao et al. [31] proposed a method known as DLBP for texture classification that utilizes most as often as possible occurring pattern structures. to obtain descriptive local texture information. But this method faces several critical limitations like lacking the concern of distant pixel connections.

This method adopts a patch steered rotation invariance approach utilizing the reference direction. It tackles the issue of discriminative pattern selection in the event of large neighbors. The method cuts down dimensionality and enhances the discerning power of feature by eliminating the superfluous feature structures. Using deference as the dominant direction the method poses certain additional advantages like it makes RLBP very quick and computationally efficient and easy. Also, classical Dominant direction follows the same calculation procedure as followed by classical LBP, hence there is no such improvement in computational complexity over classical LBP. The major drawback of this method is that only some part of the information is retained (only frequency of dominant pattern occurrence) while as pattern type information is dropped. Tno sucho overcome the above drawback another feature extraction method has been proposed that learns the most discerning and robust features from the raw input image.

v) Discriminative Complete Local Binary Pattern (DisCLBP)

To illustrate the general approach of CLBP for texture classification considering the fig below:

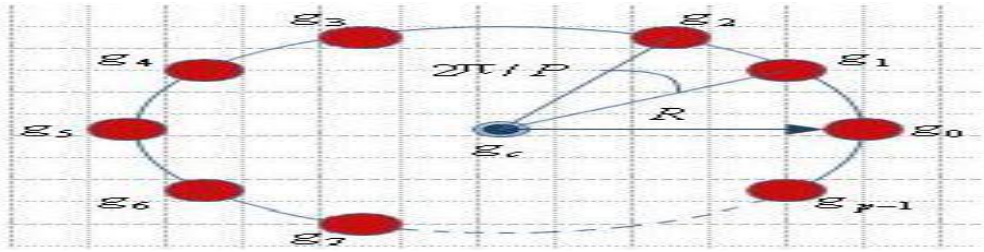

Fig. 6 P Circular neighborhood with R with central pixel and

In fig. 6 above g_c represents a central pixel and $(g_1, g_2, \cdots, g_{p-1})$ represents equally spaced circular neighborhood pixels, then, $d_p = g_p - g_c$. It gives rise to difference vector $[d_0, d_1, \ldots, d_{P-1}]$ which represents local information of image at the central pixel. Eliminating g_c prompts efficiency and illumination invariance to difference vector. Moreover, d_p can be broken down into two components. One component represents sign and another component represents magnitude. Which are given below:

$$d_p = S_p \times M_p$$

where sign component is given as :

$$S_p = \begin{cases} 1 & , \ d_p \geq 0 \\ -1 & , \ d_p < 0 \end{cases} \qquad (A)$$

and magnitude component is given by :

$$M_p = |d_p|$$

Therefore, $\left[d_0, d_1, \ldots, d_{P-1}\right] = \left[S_0, S_1, \ldots, S_{P-1}\right] \times \left[M_0, M_1, \ldots, M_{P-1}\right]$ Equation (*A*) is refeered as Local Difference Sign Magnitude Transfer (LDSTM) .

The sign component contains more local texture information as compared to the magnitude component, while a magnitude component contains, more importantly, identification information. Besides these, some more important information is present at the center. Combining all the three components leads to the capturing of both local as well as global texture information and constitutes an integral part of the LBP algorithm. To obtain more discriminative feature patterns, a 3 layered model is followed.

Layer 1: layer 1 is responsible for extracting the most prevailing and robust features from the raw input image.

Layer 2: layer 2 extracts most discriminative patterns for each class from the pool of patterns learned in the first layer.

Layer 3: layer 3 maximizes the representational capacity of features by establishing the global set of discriminative patterns, and then it encodes both the pattern frequency and pattern type information obtained from the second layer giving rise to the final feature. In this way, the DLBP by examining the frequency of occurrence of rotation invariant LBP patterns retain and most as often as possible occurring pattern structures, and discards rarely occurring patterns. In 2010 Guo et al. developed a method completed model of local binary patterns for texture classification one of the variants of LBP that uses both magnitudes of central pixel and sign of the

difference between a central pixel and its neighbors as well magnitude [32].

Advantages and Limitations:
DisLBP shows an improvement over DLBP by simply taking into consideration two properties the intra-class similarity and inter-class distance during learning. But the approach additionally experiences some basic restrictions, unable to capture non-local small texture information (micro-textures). Huge computational cost and time-consuming process due to large feature dimensions.

vi) LBP Variance (LBPV)

In 2009 Guo et al. [33] developed a method possessing rotation invariance an alternative to LBP (LBPV) property based on LBP variance with global matching that is used to signify local contrast records into 1D LBP histogram. But faces some limitations as well.

LBPV feature vector prompts much higher classification precision beyond expected values. Reduces the feature dimensionality (feature size) appreciably while keeping the performance remarkable.

vii) Local Ternary Patterns (LTP)

In 2010 Tan and Triggs [34] proposed a method known as Local Ternary Pattern (LTP) that is a generalization of the local binary pattern (LBP) and finds its application in the face recognition system under dim light conditions.

This method is discriminative to uniform regions only, Partially robust to noise.

viii) Circumferential derivative pattern operator (CD):

Unlike the traditional LBP, Wang [29] proposed a descriptor called a local circumferential derivative (CD) operator that is different from the existing descriptors and approximates tangential information for classifying texture. It takes into consideration the pixels lying on the circumference of the chosen image area to obtain tangential gradient information for texture classification. The values are threshold by taking the difference between two adjoining pixels starting from the pixel lying at an angle 0 concerning central pixel. The binary value for each pixel on the circumference is obtained by assigning a value 1 to the pixel having a value greater or equal to the comparable pixel. And a binary 0 is assigned in case the value is less than the threshold pixel. This way an 8-digit binary code is generated for each pixel on the circumference. The binary value is converted to decimal and stored as an LBP code. We obtain the feature vector for the LBP code.

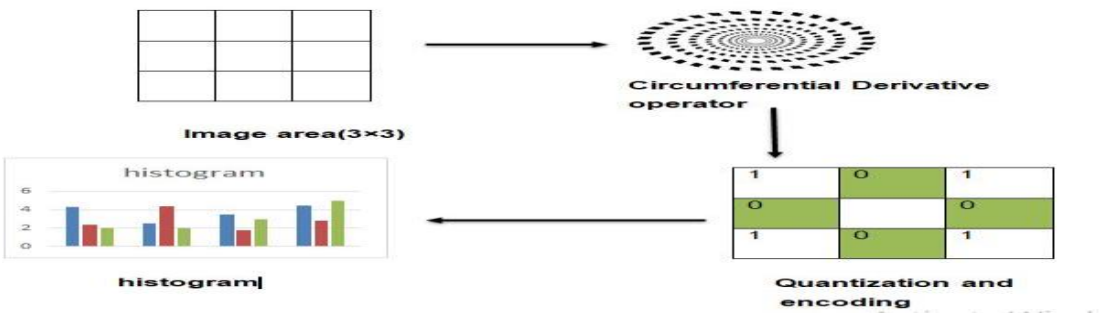

Fig. 7 Circumferential derivative operator

The mathematical formula for computing CD at a given central pixel GC and over a circular neighborhood of N pixels given a displacement of η is given as:

Using Ist order derivative

$$CD^{1}_{N,R,\eta}\left(i\right) = g_i - g_{\mathrm{mod}(i-\eta,N)}$$

Using 2nd order derivative

$$CD^{2}_{N,R,\eta}\left(i\right) = g_{\mathrm{mod}(i+\eta,N)} + g_{\mathrm{mod}(i-\eta,N)} - 2g_i$$

Unlike traditional LBP, it captures circumferential information by taking the circumference of the neighborhood of pixels. However, there is much loss of information due to lack of radial gradient information as it is only capable of capturing tangential information.

ix) Radial derivative pattern operator (RD):

Since the tangential information among the neighbors on the circumference is obtained using circumferential operators, radial-gradient information is obtained using the radial operator. Wang [43] also proposed a radial derivative (RD) operator to obtain the information of a radial gradient. The radial gradient data is obtained by computing the grey-level difference between central pixels and neighbors alongside one of the circumferential angles. We compute the gray-level difference between the pixels, by taking the summation of the pixel values lying on one circumferential angle and then take their difference with the central pixel. Finally, we save the average of the difference obtained so as not to exceed the 256-pixel values of an image. As the values obtained for three radii exceed the pixel value of the image and the image appears white, we normalize the value to 256 by taking the average of the difference. The first order radial derivative operator at a given central pixel GC is defined as:

$$RD^{1}_{N,R}\left(i\right) = g_i - g_c, \forall \;\; i = 0,1,...,N-1$$

And the second-order derivative of the radial operator is defined as:

$$RD^{2}_{N,R}\left(i\right) = g_i + g_{\mathrm{mod}(i+N/2,N)} - 2g_c$$

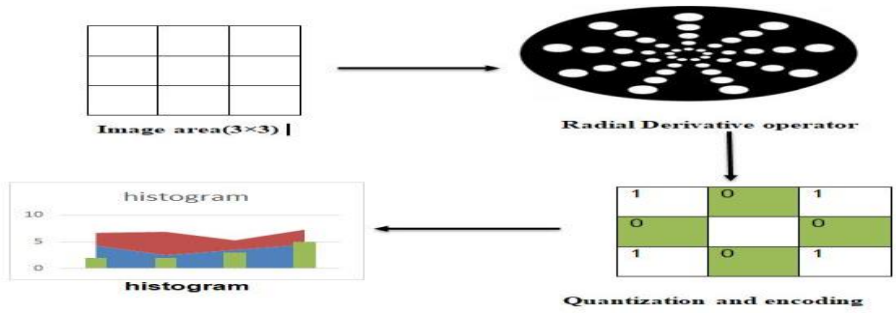

Fig.8 Radial derivative operator

Although an improvement over classical LBP of capturing radial-gradient information, it still makes a loss of tangential information due to lacking circumferential derivative operator. The radial derivative is the radial difference between a central pixel and neighboring pixel, so radial interpolation calculation between them prompts higher computational cost and memory storage. Also one of the major drawbacks of this method is that with the gradual increase in the radius from the central pixel obtained texture information among the central pixel value and the neighboring pixel value is lost which diminishes its discriminative power.

x) Concatenated Circumferential and Radial derivative pattern operator (CD $\otimes$ RD):

To obtain a more powerful and discriminative and noise-robust algorithm both the radial as well as circumferential are concatenated to each other to capture both radial gradient as well as tangential information. As the information obtained by two operators is complementary to each other we fuse both the operators to obtain the local texture information about the image. Moreover, we obtain the global texture information by incorporating the global difference (GD) operator, takes the grey-level difference among central pixel value and the average mean value of the whole image, therefore, GD operator can be combined with the CDP and RDP operator to obtain the essential texture information of the image.

$$CRDP^m = CDP^m \otimes RDP^m \otimes GD$$

$\otimes$ histogram concatenation operator.

Where *m* denotes the order of derivative, and

$$GD(p_c) = s(g_c - \mu_p)$$

Where, μ_p represents mean grey-value of the image.

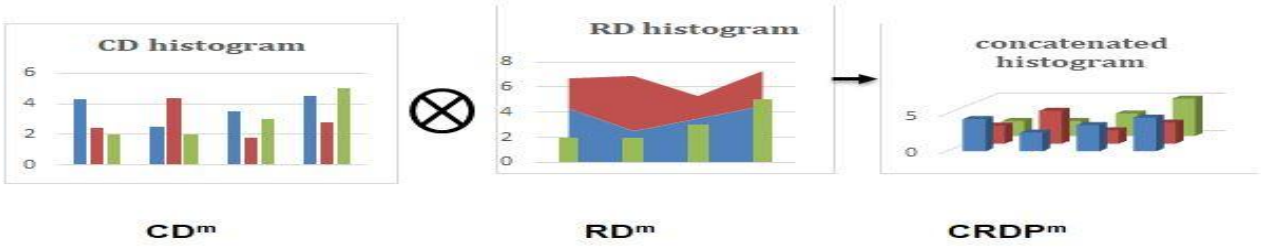

Fig. 9 Concatenated RD and CD

The concatenation of both operators helps in capturing both local as well as global texture information using central difference operator. But this method still it suffers from some critical limitations as radial interpolation calculation prompts huge computational cost and increased memory usage. At times it leads to spatial information lost which degrades its performance and discriminative power.

xi) Adaptive Concatenated Circumferential and Radial derivative pattern operator $(\mathbf{CD} \otimes \mathbf{RD})$:

Unlike all existing LBP descriptors, Wang proposed a descriptor that processes tangential information for texture classification. Based upon different scales, positions and number of neighborhood pixels, various descriptors can be defined for a given central pixel. Based upon the same principles circumferential texture information is obtained using CD operator. The new adaptive CD (ACD) operator is adaptive to change in radius $R = 3$. This adaptiveness to radius makes the ACD operator more robust to noise and discriminative. The mathematical formulation of ACD operator at a given central pixel g_c for its kth neighborhood is given by:

$$ACD^1_{P,R,\beta}(k) = g_k - g_{\mathrm{mod}(k-\beta,P)}$$

Where, *P* denotes the neighboring pixels on the circular neighborhood of radius *R*. $\beta = 1, 2, \ldots, \frac{P}{2}$ refers to the circumferential displacement about circumferential angle $\theta = \frac{2\pi}{P}, 2\left(\frac{2\pi}{P}\right), \ldots, \pi$. Similarly, any higher-order derivative can be determined for the CD operator for different values of(P, R). Assuming j is even, the j[th] order derivative of the circumferential operator is given as:

$$ACD^j_{P,R,\beta}(k) = \sum_{i=0}^{k} (-1)^k \binom{j}{i} g_{\mathrm{mod}\left(k+\left(\frac{k}{2}-i\right)\beta,P\right)}$$

The adaptive circumferential derivative pattern (ACDP) utilizes the ACD operator and (ARD) operator utilized by an adaptive radial derivative pattern (ARDP). The development of ACDP and ARDP descriptors show resemblance with classical LBP apart from the use of another operator. Formally, we define ACDP and ARDP codes at g_c as where g_c represents a central pixel.

$$ACDP^{j}_{P,R,\beta}(k)=\sum_{k=0}^{P-1}s\left(ACD^{j}_{P,R,\beta}(k)\right)\cdot 2^{k} \qquad (1)\ ARDP^{j}_{P,R}=\sum_{k=0}^{P-1}s\left(ARD^{j}_{P,R}(k)\right)\cdot 2^{k}$$

Where, P is the count of pixels in the circular neighborhood of radius R around the central pixel, j is the order of derivative. From equation (1) it can be seen that both the $ACDP^{j}_{P,R,\beta}$ and $ARDP^{j}_{P,R}$ are capable of recognizing 2^{P} distinguished binary patterns.

Advantages and Limitations:

Both the descriptors are robust to monotonic grayscale variations but are not rotation invariant and the dimensions of the histogram produced are high. Some of the modifications are proposed to overcome the drawbacks.

Rotation invariance: LBP is invariant to rotation as a similar texture image can be represented by more than one angle. We introduce rotation invariance to ACDP and ARDP codes at g_c is given by:

Where g_c represents the corresponding central pixel. $ACDP^{j,ri}_{P,R,\beta}=\min\left\{R\circ R\left(ACDP^{j}_{P,R,\beta}(k),k\right)\right\}$

$$ARDP^{j,ri}_{P,R}=\min\left\{R\circ R\left(ARDP^{j}_{P,R}(k),k\right)\right\}$$

Where, $R\circ R(x,k)$ performs a bitwise right circular shift k times on the P-bit number x. Then a final rotation invariant feature vector of an image is obtained by applying $\left(ACDP^{j,ri}_{P,R,\beta}\ ,\ ARDP^{j,ri}_{P,R}\right)$ codes to every pixel in an image and corresponding feature vector (histogram) of these codes are constructed.

Reducing feature dimensionality: The uniformity measure is outlined as:

$$U(LBP_{P,R})=\left|s(t_{P-1}-t_c)-s(t_0-t_c)\right|+\sum_{p=1}^{P-1}\left|s(t_p-t_c)-s(t_{p-1}-t_c)\right| \qquad (2)$$

Rotation invariant uniform patterns have got the uniformity of two or less and are defined as:

$$LBP^{riu2}_{P,R}=\begin{cases}\sum_{p=0}^{P-1}s\left(t_p-t_c\right)\cdot 2^{p}\ ;\text{if } U\left(LBP\right)_{P,R}\le 2\\ P+1 \qquad\qquad ;\text{otherwise}\end{cases} \qquad (3)$$

We apply uniform representation of LBP [29] to reduce the dimensions of rotation invariant ACDP and ARDP descriptors. As the uniformity measure is defined in equation (2) and (3). Therefore, on similar lines, the rotation invariant uniform *ACDP* code (for uniformity of almost 2) is defined as:

$$ACDP^{j,riu2}_{P,R,\beta}$$

$$=\begin{cases}\sum_{k=0}^{P-1}s\left(ACDP^{j,ri}_{P,R,\beta}(k)\right);\text{if } U\left(ACDP^{j,ri}_{P,R,\beta}(k)\right)\le 2\\ P+1 \qquad\qquad ;\text{otherwise}\end{cases}$$

Similarly, the rotation invariant uniform ARDP code (for uniformity of almost 2) is defined as:

$$ARDP^{j,riu2}_{P,R,\beta}$$

$$=\begin{cases}\sum_{k=0}^{P-1}s\left(ARDP^{j,ri}_{P,R,\beta}(k)\right);\text{if } U\left(ARDP^{j,ri}_{P,R,\beta}(k)\right)\le 2\\ P+1 \qquad\qquad ;\text{otherwise}\end{cases}$$

By applying rotation invariance and uniformity measure, the feature dimensions reduce from 2^{P} value to P+2 bins, which is considerable reduction. Since the information captured by the two rotation invariant operators above is complementary, we fuse both the operators to obtain the local texture information about the image. Moreover, we obtain the global texture

information by incorporating the global difference (GD) which is the gray-level difference between (g_c) and (ϑ_p), where g_c represents central pixel and ϑ_p represents the average mean value of the whole image. We, therefore, combine the GD operator with the ACDP and ARDP operator to obtain the essential texture information of the image in a concatenated operator. Adaptive circumferential and radial derivative pattern (ACRDP) operator, defined as :

$$ACRDP^j = ACDP^j \otimes ARDP^j \otimes GD^j$$

Where,

- $\otimes$ is the joint histogram operator.
- j is the order of derivative, and
- $GD_{P_c} = s(g_c - \vartheta_p)$ is the global difference operator.

xii) Various other LBP variants

In 2009 M Heikkila et al. [35] proposed a descriptor **(CS-LBP)** that is a modification over classical LBP employs center symmetric local binary pattern. But the drawback of this method is as it loses significance over LBP in object category classification.

In 2011 Lee et al. proposed a method Local color vector binary pattern **(LCVBP)** that is the color based descriptor for face recognition. But the method faces computational limitation as it is computationally infeasible [36].

In 2013 Rouzebeh et al. devised Local frequency descriptor (LFD) for texture classification, the method is noise-robust and rotation invariant but there is a tradeoff between filtering area and robustness of the method [37].

In 2014 (Vinh et al) proposed a model known as support local binary pattern **(SLBP)** to establish a relationship among different pixels in the local region. But these methods need to be modified to achieve noise robustness and rotation invariance [38].

In 2014 QI et al. Proposed a method known as pairwise rotation invariant binary pattern **(PRICOLBP)** feature to introduce multi-scale, multi-orientation and multi-channel information. But the method is incapable to give remarkable classification performance on multiple features against a single feature [39].

In 2014 Liu et al. devised a technique known as Binary rotation invariant and noise-tolerant **(BRINT)** texture classification method for multi-scale and multi-resolution information. But the methods face some limitations that it is only limited to texture classification and is not able to perform face or object recognition properly [40].

In 2015 (Ryu et al) proposed a method known as the sorted consecutive local binary pattern **(LBP)** for texture classification that can encode the patterns regardless of their spatial transition. But the method prompts computational cost because of the tedious task of dictionary learning [41].

In 2015 (Hafiene et al) developed a method Adaptive median binary patterns **(AMBP)** for texture classification, it extends the Median binary pattern texture feature. Adopt a nonparametric learning methodology. But the method performs best only for the impulsive noise and is quite sensitive to the rest of the types of noise [42]. Summary of
LBP variants and challenged posed by these descriptors are given in the table 4 at the end of the Results and discussions section.

III. Experimental evaluation

Total of 10 LBP variants are implemented on two different databases to evaluate the performance I terms of both classification accuracy as well as computational efficiency. The detailes description of datasets used for the experiment are as given as below.

A) Dataset Discription:

i) 2D HeLa :Publicly accessible 2D HeLa [44] is used in this paper. The dataset contains fluorescence microscopic images of HeLa cells maculated with different fluorescent dyes as per the specification of the various organelles present in the dataset. It contains 10 distinct organelles given in the table below with a detailed description like the total number of classes in the dataset and the number of samples presents per class.

Table 1: 2-D HeLa dataset description

S. No.	Class	2-D heLa dataset
1	Actin-Filaments	90
2	Endosome	84
3	ER	86
4	Golgi	87
5	Giantin	85
6	Golgi-GPP1308Lysome	91
7	Microtubules	73
8	Mitochondria	80
9	Nucleolus	87
10	Nucleus	62
Total		862

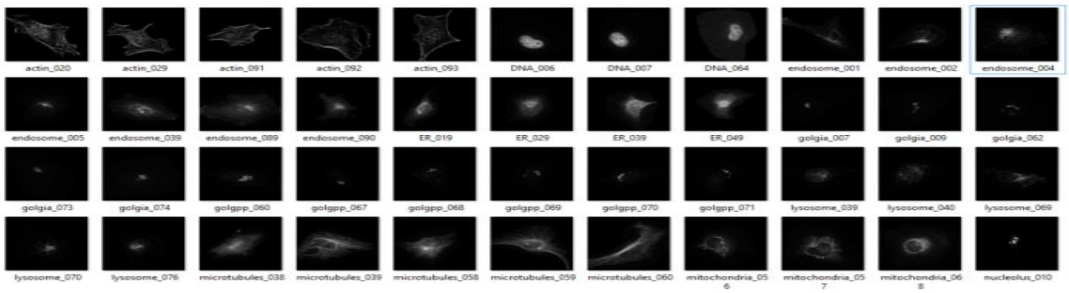

Fig. 10: 2D HeLa sample dataset

The whole dataset which is internally divided into 10 classes is divided into two classes training class consists of 521 training samples and test classes consist of a total of 341 samples. Each of the texture images in the testing set was subjected to 3 different rotations (100, 300, and 450). While the images in the training set are original. i.e., with an angular. Rotation of 00. The results are given in Table 3 and the classification accuracy is measured with two metrics which are chi-square and Euclidean distance. The characteristic of the dataset is given in the table below.

Table 2: Summary of 2–D HeLa Database

Dataset	***2-D HeLa***
Classes	10
Images per class	Varied
Train samples	521
Test samples	341
Total samples	862
Image size	382×382
Rotation	Yes
Illumination changes	Yes

ii) KIMIA PATH 960: Twenty scans that visually characterize pattern types from KIMIA PATH 960 [45] are carefully chosen from an array of 400 slide images containing epithelial, muscle and connective tissue. 48 ROI of the same size is manually nominated from each WSI and down-sampled to 308×168 patches. Hence, a dataset of 960(= 20× 48) images is acquired as shown in fig. below. The whole data set of 960 histopathology images is divided into two categories training images of twenty different classes class A class B so on till class T, each training class consists of 40 images each. And out of whole dataset 160 images are kept as testing images and internally divided into twenty classes, each class consists of 8 images.

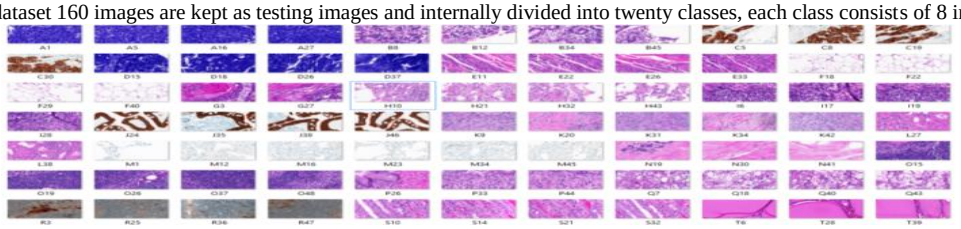

Fig 11. KIMIA PATH 960 sample dataset

Whole dataset which is internally divided into 10 classes is divided into two classes training class consists of 521 training samples and test classes consists of total 341 samples. Each of the texture images in testing set was subjected to 3 different rotations (100, 300, and 450). While the images in training set are original. i.e., with an angular rotation of 00. The characteristic of the dataset is given in the table below.

S.No	***Dataset***	***Description***
1	Classes	20
2	Images per class	40
3	Train samples	800
4	Test samples	160
5	Total samples	960
6	Image size	308×168

7	Rotation	Yes
8	Illumination Changes	Yes

Table 3: Summary of KIMIA PATH 960 Database

In the experiment , we consider both databases separately unlikely other traditional methods which considers the (R,P) as (1,8),(2,16),(3,24). We test all the possible combination of R and P. The radius value are chosen as R =1, 2, 3 and number of neighbors as p=8,12,16 with the large value of radius no improvement was shown so highest value of R was set to 3. And the values of P is restricted to 16.If the values are increased beyond 16.It will lead to considerable gain in the dimensionality an computation complexity without any significant progress. Among earler LBP versions $R_iLBP,\ R_iLBPU$ chieves high accuracy of 93% and 90% for $R=3, and\ \ P=16$ .The performance evaluation of all the variants of LBP including LBP itself on both the datasets using two dissimilarity metric are given below.

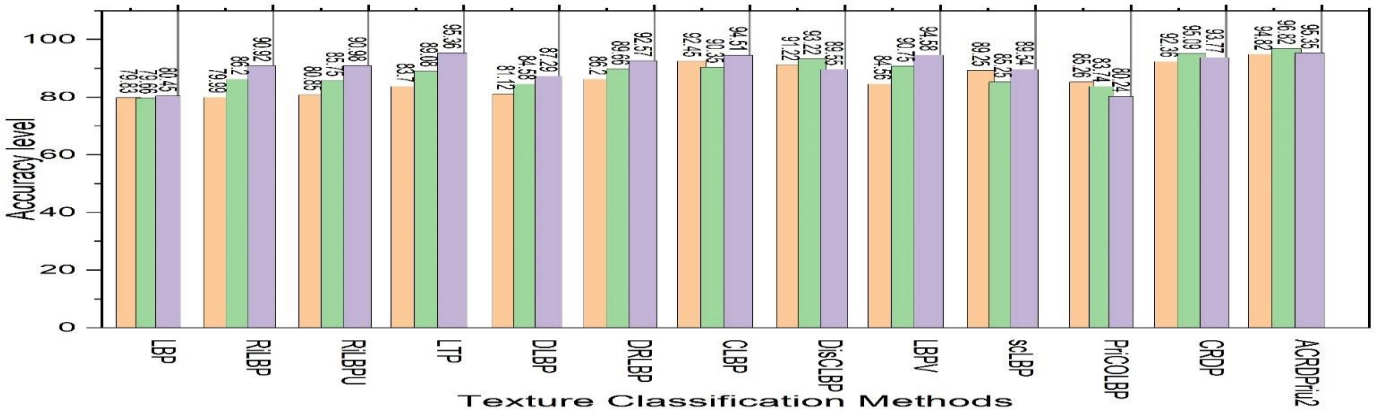

Fig 12. Classification accuracy using chi-square distance on 2D Hela

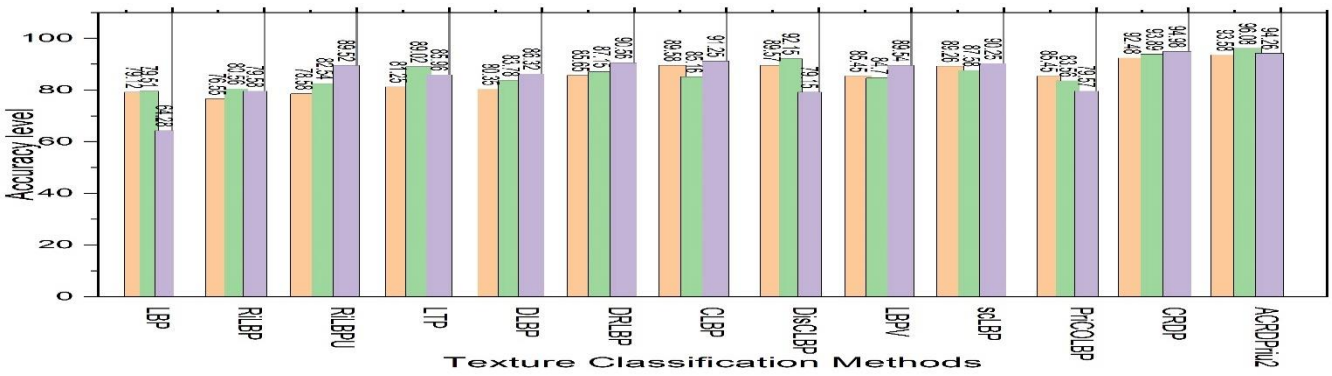

Fig 13. Classification accuracy using L_2 -norm distance on 2D Hela

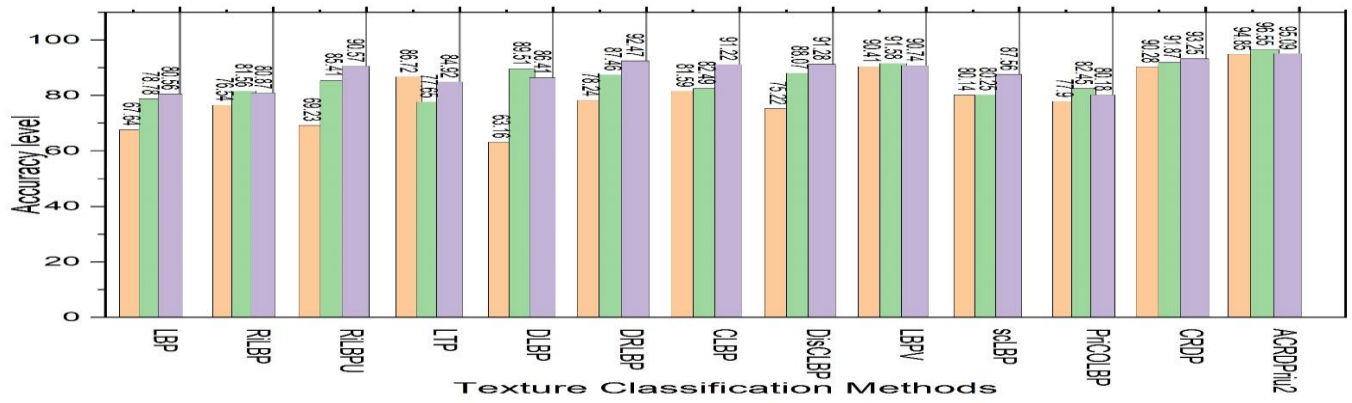

Fig 14. Classification accuracy using L_2 -norm distance on KIMIA PATH 960

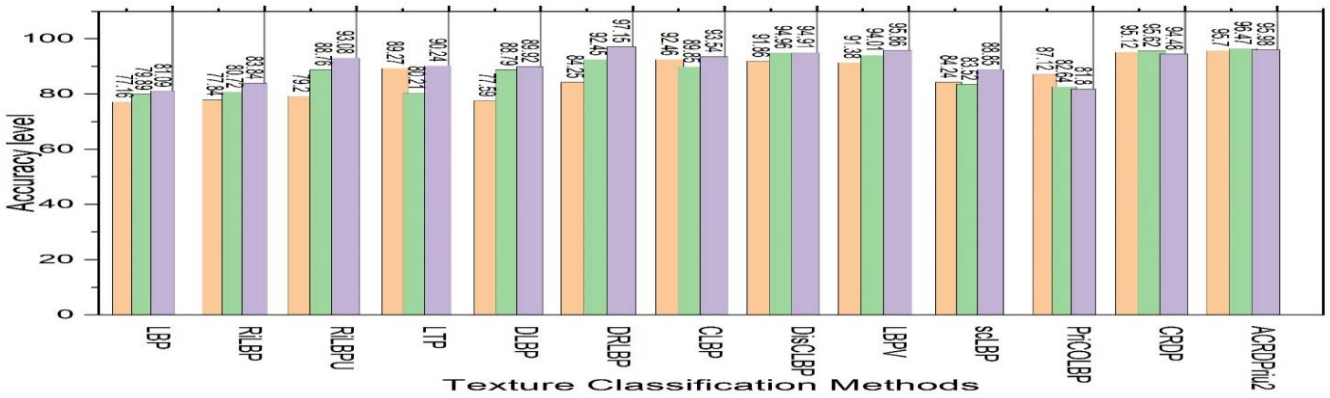

Fig 15. Classification accuracy using L_2 -norm distance on KIMIA PATH 960

IV) Computational time analysis

To assess the computational load of different LBP variants, computation time (in a sec) for feature extraction comparison is done for both training and testing on the user database and the values are recorded in Table 5 and 6. As the number of neighboring pixels and radii increases, the CPU time for computation increases for each descriptor, but down the table, an improvement in CPU time is experienced about added functionality in each descriptor Computational time performance in seconds for feature extraction, training, and testing for one image on a dataset is given by graphs below.

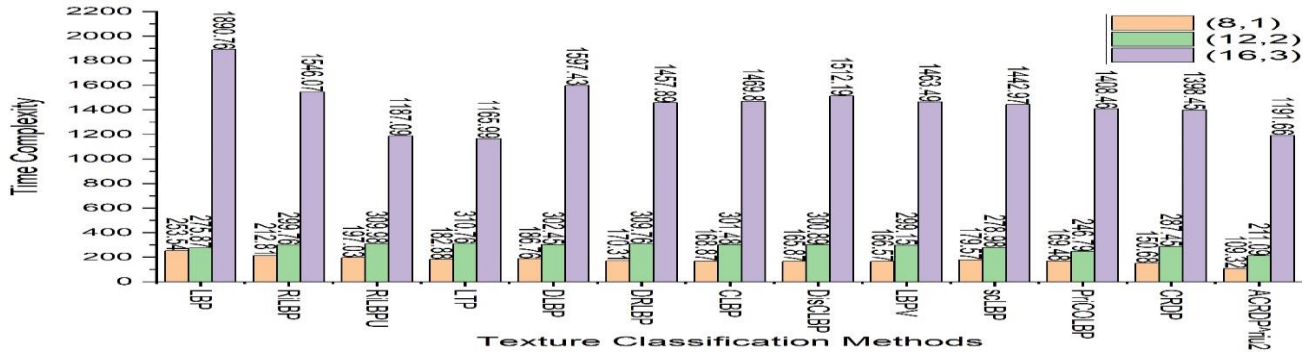

Fig 16. Time complexity computation using KIMIA PATH 960

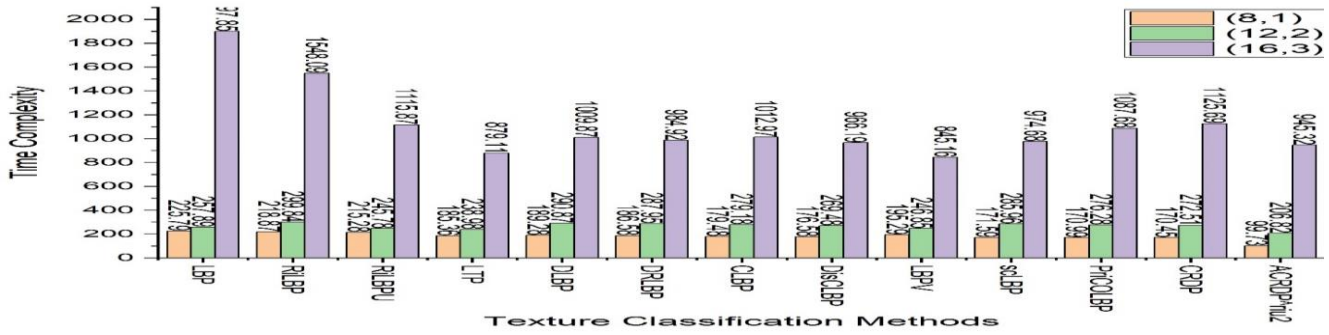

Fig 17. Time complexity computation using KIMIA PATH 960

Results from above graphs clearly demonstrate Adaptive circumferential and radial derivative LBP operator outperforms all the other existing methods in classification accuracy and also is computationally efficient. These results validate the supposition that an improved result is obtained by fusing both the radial and circumferential information to the LBP descriptor.

IV) Conclusion and future work

The paper provides complete description of Local Binary pattern and it's all existing as well as recent variants. The advantages and disadvantages of thee variants are discusses as well. Performance evaluation of all these variants using two publicly available databases KIMIA PATH 960 and 2D-HeLa. Implementation of these variants on these database shows that among all the LBP variants adaptive circumferential and radial derivative operator outperforms all n terms of both classification accuracy as well as computational time complexity. To evaluate classification accuracy two distance metrics has been used Chi square distance and L2 norm distance metric.

Future challenges: In order to improve the classification and recognition accuracy further deep learning method like can be implemented, which also eliminates the need of hand crafted feature extraction. CNN automatically performs feature extraction process directly from raw input data. And we can further implement the transfer learning concept in deep learning to make the process computationally more efficient and decrease the training time. LBP can be also combined with CNN to improve the performance of classification.

Table 4. Summary of LBP varinats is given by the table as below

S.No	Texture method	Description	Challenges
1	**Local Binary Patterns (LBP)**	Texture description methods involving 3×3 neighborhood and concept of threshold for extraction of textures from input raw images.	• Low computational complexity • Generates devastatingly large histograms which prompts higher utilization of memory
2	**Local ternary Patterns (LTP)**	Generalization of LBP used for texture extraction under dim lighting conditions.	• Least robustness towards noise and image aberrations. • Finds its application to uniform regions only.
3	**LBP variance (LBPV)**	Modified and alternative version of LBP based on LBP variance in order to obtain local contrast information using 1D histogram.	• Degradation of overall performance while reducing the feature dimensionality of the input raw data. • Acquiring classification precision rate beyond expect values.
4	**Local color vector binary pattern (LCVBP)**	LBP variant based on color based descriptor particularly used for facial recognition.	• Huge computational complexity.

5	**Completed Local Binary Pattern (CLBP)**	Completed model of LBP using both sign and magnitude of difference between central and neighboring pixel. Sign component represents local texture information while more specific information is present in magnitude component.	• The method is not able capture the non-local micro textures. • Time consuming due to huge feature size.
6	**Center symmetric Local binary pattern (CS-LBP)**	Modification to LBP using center symmetry for LBP features extraction.	• Loses significance over LBP in object classification and detection.
7	**Support Local Binary Pattern (SLBP)**	The method is utilized for extraction of features in multi-scale, multi-orientation, multi-channel information.	• Degradation of classification performance on multiple features against single feature.
8	**Binary rotation invariant and noise tolerant feature extraction method (BRINT)**	The method is particularly used for multi-scale, multi-resolution information.	• Specific for texture classification and fails for object detection and classification.
9	**Adaptive median binary patterns (AMBP)**	This method makes utilization of median binary patterns for texture extraction.	• Greater sensitiveness towards noises except impulsive noise.
10	**Local circumferential and radial derivative pattern** $(CD \otimes RD))$	Implements both circumferential as well as radial derivative pattern for texture classification.	• Performs well for all types of noise except multiplicative noise.

VI. REFRENCES

[1] M. Tuceryan and A. K. Jain, ``Texture analysis," in *The Handbook ofPattern Recognition and Computer Vision*, 2nd ed., C. H. Chen, L. F. Pau,and P. S. P. Wang, Eds. Singapore: World Scientific, 1998.
[2] S.Y. Lu and K. S. Fu, ``Asyntactic approach to texture analysis," *Comput.Graph. Image Process.*, vol. 7, no. 3, pp. 303-330, 1978.

[3] R. W. Ehrich and J. P. Foith, ``A view of texture topology and texturedescription," *Comput. Graph. Image Process.*, vol. 8, no. 2, pp. 174-202, 1978.
[4] L. Carlucci, ``A formal system for texture languages," *Pattern Recognit.*, vol. 4, no. 1, pp. 53-72, 1972.

[5] B. Kjell and C. R. Dyer, "Edge separation and orientation texture measures,'' Dept. Comput. Sci., Univ. Wisconsin-Madison, Madison, WI, USA, Tech. Rep. 559, 1984.

[6] F. M. Vilnrotter, R. Nevatia, and K. E. Price, "Structural analysis ofnatural textures," *IEEE Trans. Pattern Anal. Mach. Intell.*, vol. PAMI-8, no. 1, pp. 76-89, Jan. 1986.

[7] S. Lazebnik, C. Schmid, and J. Ponce, "A sparse texture representationusing local affine regions," IEEE Trans. Pattern Anal. Mach. Intell.,vol. 27, no. 8, pp. 1265-1278, Aug. 2005.

[8] T. Chalumeau, L. D. F. Costa, O. Laligant, and F. Meriaudeau, "Complex networks: application for texture characterization and classification," Electron. Lett. Comput. Vis. Image Anal., vol. 7, no. 3, pp. 93-100, 2009.

[9] N. Ahuja and A. Rosenfeld, "Mosaic models for textures," IEEE Trans.Pattern Anal. Mach. Intell., vol. PAMI-3, no. 1, pp. 1-11, Jan. 1981.

[10] K. B. Eom, "Segmentation of monochrome and color textures using moving average modeling approach," Image Vis. Comput., vol. 17, nos. 3-4, pp. 233-244, 1999.

[11] R. L. Kashyap, R. Chellappa, and A. Khotanzad, “Texture classification using features derived from random field models,” Pattern Recognition. Lett., vol. 1, no. 1, pp. 43-50, 1982.

[12] N. Ahuja and A. Rosenfeld, “Mosaic models for textures,” IEEE Trans. Pattern Anal. Mach. Intell., vol. PAMI-3, no. 1, pp. 1-11, Jan. 1981.

[13] D. Gabor, “Theory of communication. Part 1” The analysis of information’s. Inst. Elect. Eng. III, Radio Commun. Eng., vol. 93, no. 26,pp. 429-441, Nov. 1946.

[14] J. He, H. Ji, and X. Yang, “Rotation invariant texture descriptor using local shearlet-based energy histograms,” IEEE Signal Process. Lett.,vol. 20, no. 9, pp. 905-908, Sep. 2013.

[15] R. Shenbagavalli and K. Ramar, “Classification of soil textures based on laws features extracted from preprocessing images on sequential and random windows,” Bonfring Int. J. Adv. Image Process., vol. 1, pp. 15-18, Dec. 2011.

[16] Y. Dong, J. Feng, L. Liang, L. Zheng, and Q. Wu, “Multiscale sampling based texture image classification,” IEEE Signal Process. Lett., vol. 24, no. 5, pp. 614-618, May 2017.

[17] P.Yang, F. Zhang, and G.Yang, “Fusing DTCWT and LBP based features for rotation, illumination and scale invariant texture classification,” IEEE Access, vol. 6, pp. 13336-13349, 2018.

[18] E. E. A. Abusham and H. K. Bashir, “Face recognition using local graph structure (LGS),” in Proc. Int. Conf. Hum.-Comput. Interact. Berlin, Germany: Springer, Jul. 2011, pp. 169-175.

[19] A. S. Al-Shibli and E. Abusham, “Face recognition using local graph structure and support vector machine (LGS-SVM),” Int. J. Comput. Appl.
Sci., vol. 2, no. 2, pp. 68-72, 2017.
[20] A. R. Backes, A. S. Martinez, and O. M. Bruno, “Texture analysis using graphs generated by deterministic partially self-avoiding walks,” Pattern Recognit., vol. 44, no. 8, pp. 1684-1689, 2011.

[21] J. J. de Mesquita Sá Junior, A. R. Backes, and P. C. Cortez, “Texture analysis and classi_cation using shortest paths in graphs,” Pattern Recognit. Lett., vol. 34, no. 11, pp. 1314-1319, 2013.

[22] M. Crosier and L. D. Griffin, “Using basic image features for texture classification,” Int. J. Comput. Vis., vol. 88, no. 3, pp. 447-460, 2010.

[23] J. Zhang, H. Zhao, and J. Liang, ``Continuous rotation invariant local descriptors for texton dictionary-based texture classification," Comput. Vis. Image Understand., vol. 117, no. 1, pp. 56-75, 2013.

[24] V. Andrearczyk, “Deep learning for texture and dynamic texture analysis,” Ph.D. dissertation, School Electron. Eng., Dublin City Univ., Dublin, Republic of Ireland, 2017.

[25] V. Andrearczyk and P. F. Whelan, “Using _lter banks in convolutional neural networks for texture classification,” *Pattern Recognit. Lett.,* vol. 84, pp. 63-69, Dec. 2016.

[26] V. Andrearczyk and P. F. Whelan, “Convolutional neural network on three orthogonal planes for dynamic texture classification,” *Pattern Recognit.,* vol. 76, pp. 36-49, Apr. 2018.

[27] J.-R. Yeh, C.-W. Lin, and J.-S. Shieh, “An approach of multiscale complexity in texture analysis of lymphomas,” IEEE Signal Process. Lett., vol. 18, no. 4, pp. 239-242, Apr. 2011.

[28] L. E. V. Silva, A. C. S. S. Filho, V. P. S. Fazan, J. C. Felipe, and J. J. de Mesquita Sá Junior, “Two-dimensional sample entropy: Assessing image texture through irregularity,” *Biomed. Phys. Eng. Express*, vol. 2, no. 4, p. 045002, 2016.

[29] Ojala, T., Pietikainen, M., & Maenpaa, T. (2002). Multiresolution gray-scale and rotation invariant texture classification with local binary patterns. IEEE Transactions on pattern analysis and machine intelligence, 24(7), 971-987.

[41] Mehta, R., & Egiazarian, K.O. (2016). Dominant
Rotated Local Binary Patterns (DRLBP) for texture classification. *Pattern Recognition Letters, 71*, 16-22.

[31] Liao, S., Law, M. W., & Chung, A. C. (2009).
Dominant local binary patterns for texture classification. IEEE transactions on image processing, 18(5), 1107-1118.

[32] Guo, Z., Zhang, L., & Zhang, D. (2010). A Completed Model of local binary pattern operator for texture classification. IEEE Transactions on Image Processing, 19(6), 1657-1663.

[33] Guo, Z., Zhang, L., & Zhang, D. (2010). Rotation invariant texture classification using LBP variance (LBPV) with global matching. Pattern recognition, 43(3), 706-719.

[34]Tan, X., & Triggs, B. (2010). Enhanced local texture feature sets for face recognition under difficult lighting conditions. IEEE transactions on image processing, 19(6), 1635-1650.

[35] Heikkilä, M., Pietikäinen, M., & Schmid, C.
(2009). Description of interest regions with local binary patterns. Pattern recognition, 42(3), 425-436.

[36] Lee, S. H., Choi, J. Y., Plataniotis, K. N., & Ro,
Y. M. (2011, September). Local color vector binary pattern for face recognition. In Image Processing (ICIP), 2011 18th IEEE International Conference on pp. 2997-3000, IEEE.

[39] Qi, X., Xiao, R., Li, C. G., Qiao, Y., Guo, J., &
Tang, X. (2014). Pairwise rotation invariant co-occurrence local binary pattern. IEEE Transactions on Pattern Analysis and Machine Intelligence, vol. 36, no. 11, pp. 2199-2213.

[40] Liu, L., Long, Y., Fieguth, P. W., Lao, S., &
Zhao, G. (2014). BRINT: binary rotation invariant and noise tolerant texture classification. IEEE Transactions on Image Processing, 23(7), 3071-3084.

[41] Ryu, J., Hong, S., & Yang, H. S. (2015). Sorted
consecutive local binary pattern for texture classification. IEEE Transactions on Image Processing, 24(7), 2254-2265.

[42] Hafiane, A., Palaniappan, K., & Seetharaman, G. (2015). Joint adaptive median binary patterns for texture classification. Pattern Recognition, 48(8), 2609-2620.

[43] Wang, K., Bichot, C. E., Li, Y., & Li, B. (2017).Local binary circumferential and radial derivative pattern for texture classification. Pattern Recognition, 67, 213-229.

[44]https://ome.grc.nia.nih.gov/iicbu2008/hela/index.html.

[45].http://kimia.uwaterloo.ca/kimia_lab_data_Path960.html